communications earth & environment

Article

A Nature Portfolio journal

https://doi.org/10.1038/s43247-026-03736-0

Nitrogen limitation amplifies future warming by weakening terrestrial carbon cycle feedbacks and sink capacity

Check for updates

Gang Tang [1,2] ✉, Zebedee Nicholls[3], Alexander Norton[4], Thomas Gasser [3], Tilo Ziehn [4], Sönke Zaehle [2] & Malte Meinshausen [1]

The inclusion of the terrestrial nitrogen cycle in Earth system models (ESMs) represents a major advance, yet its role in fully coupled climate–carbon–nitrogen dynamics remains underexplored. Using MAGICC-CNit to emulate CMIP6 ESMs, we present the first emission-driven, probabilistic cross-ESM projections of climate–carbon–nitrogen interactions and global carbon budgets across SSP1-2.6 to SSP5-8.5 scenarios. Nitrogen limitation weakens the carbon–concentration feedback by 37% (from 1.10 ± 0.36 to 0.70 ± 0.37 GtC ppm^{-1}) and the carbon–climate feedback by 16% (from -53.35 ± 37.53 to -44.6 ± 30.1 GtC °C^{-1}), reducing land carbon uptake (18-54%) and increasing atmospheric CO_2 ($+15$–57 ppm) and global warming ($+0.16$–0.25 °C) by 2100, with high-emission scenarios risking land becoming a net carbon source. Carbon-only ESMs implicitly capture nitrogen constraints historically but not future impacts, reinforcing the need for explicit coupling. These findings provide an internally consistent quantification of nitrogen's role in coupled climate–carbon dynamics across ESMs and scenarios, highlighting the value of physically based emulators as a self-consistent framework for advancing projections.

It is widely acknowledged from both experiments and models that nutrients, especially nitrogen, are a significant constraint for the carbon cycle and therefore will influence the future climate[1–4]. Many carbon-nitrogen coupled models have performed "nitrogen-on" vs. "nitrogen-off" experiments to isolate the role of nitrogen in different processes (i.e., the same model and parameterizations, with nitrogen constraints on carbon dynamics enabled or disabled)[2,5–8]. Nevertheless, two key challenges remain in quantifying nitrogen's role in the coupled carbon–climate system. First, most models have been run in an "offline" configuration with prescribed climate and CO_2 concentrations, leaving the nitrogen feedback effect on future climate projections unassessed. Second, even under these idealized offline conditions, models display a wide range of responses to nitrogen[7,9], underscoring substantial uncertainties.

The first challenge is partly addressed by Earth system models (ESMs), which explicitly couple the carbon-nitrogen cycle with the climate system[10]. For example, comparisons of ESMs with and without nitrogen cycles in the Coupled Model Intercomparison Project Phase 6 (CMIP6) indicate that including nitrogen improves the simulation of carbon cycle dynamics[11,12]. Yet, such comparisons do not isolate nitrogen effects within the same ESM, conflating differences in model structure with nitrogen inclusion. Moreover, CMIP6 largely relies on concentration-driven experiments with prescribed CO_2, restricting representation of climate–carbon cycle feedbacks[13,14]. The explicit quantification of net climate effect would involve emission-driven, fully coupled ESMs with systematic sensitivity analyses and internal variability quantification under nitrogen-on and nitrogen-off configurations for each ESM. However, such experiments remain computationally prohibitive and technically challenging, partially because they require different pre-industrial spin-ups to equilibrium conditions in ESMs.

The second challenge—large inter-model spread—persists and even amplifies when climate-carbon-nitrogen interactions are represented in ESMs. This reflects both limited process-level understanding and insufficient observational constraints for model evaluation[9,15–18] and highlights the need for an ensemble approach to appropriately quantify the effects of land carbon-nitrogen coupling on the future carbon–climate system[7].

Our recent work partially resolves both challenges: using CNit, a unified framework with demonstrated emulation performance for the majority of CMIP6 ESMs, we have synthesized and quantified the magnitude and uncertainty of nitrogen effects represented in state-of-the-art

[1]School of Geography, Earth and Atmospheric Sciences, The University of Melbourne, Melbourne, VIC, Australia. [2]Department of Biogeochemical Signals, Max Planck Institute for Biogeochemistry, Jena, Germany. [3]Energy, Climate and Environment (ECE) Program, International Institute for Applied Systems Analysis (IIASA), Laxenburg, Austria. [4]CSIRO Environment, Aspendale, VIC, Australia. ✉e-mail: gang.tang.au@gmail.com; gang.tang@student.unimelb.edu.au; tgang@bgc-jena.mpg.de

ESMs[19,20]. Yet, the critical next step—quantifying how these nitrogen constraints dynamically interact with the climate and carbon cycle within fully coupled, emission-driven projections—remains unexplored. To bridge this gap, we use MAGICC-CNit (Model for the Assessment of Greenhouse Gas Induced Climate Change v7.5.3 with CNit v2.0)[19–21] for emission-driven, probabilistic ensemble projections of the climate and carbon cycle under the scenarios in CMIP6 ScenarioMIP[14,22]. To isolate nitrogen effects, we draw on a consistent climate ensemble[23,24] and pair it with different carbon cycle representations: the MAGc ensemble (emulated C-only ESMs), the MAGcn ensemble (emulated CN-coupled ESMs), and the MAGcnoff ensemble (emulated CN-coupled ESMs in which nitrogen does not affect carbon dynamics, see Methods). Together, these ensembles synthesize current ESM uncertainties regarding nitrogen, trace their impacts on fully coupled climate–carbon cycle projections, and provide probabilistic insights into future pathways while elucidating the critical role of nitrogen.

Results

Future warming levels and atmospheric CO_2 concentrations under SSPs

Across all SSPs, the MAGcn ensemble projects consistently higher median GSAT anomalies (hereafter "warming") than MAGcnoff, while MAGc produces slightly greater warming than MAGcnoff throughout the century (Fig. 1a). The warming differences between MAGcn and MAGcnoff (and MAGc) increase over time. A similar pattern appears for atmospheric CO_2 concentrations (Fig. 1b); however, the median values of MAGcnoff and MAGc converge under SSP3-7.0 and SSP5-8.5. The ensemble 5th–95th percentiles also maintain the ordering MAGcn > MAGc > MAGcnoff throughout the projection period for both GSAT and CO_2 concentrations (Supplementary Fig. S1).

By 2100, the MAGcn ensemble projects GSAT anomalies (median [5th–95th percentile]) of 1.74 [1.17, 2.62] °C for SSP1-2.6, 2.80 [2.00, 3.96] °C for SSP2-4.5, 4.09 [3.12, 5.54] °C for SSP3-7.0, and 5.08 [3.75, 7.07] °C for

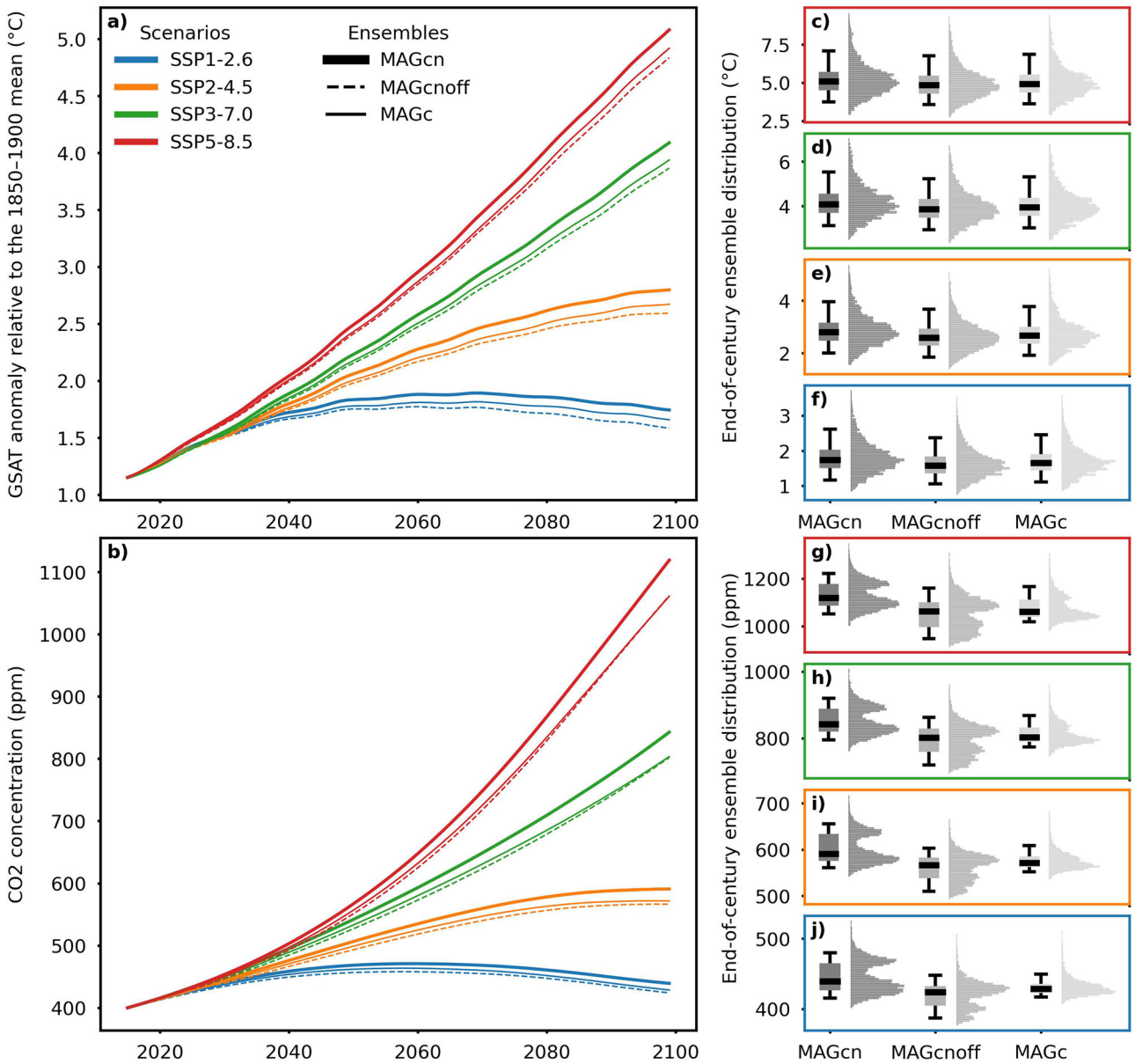

Fig. 1 | Projected global surface air temperature (GSAT) anomalies relative to the 1850–1900 mean and atmospheric CO_2 concentrations from the MAGICC-CNit ensembles under different SSP scenarios. The left panels show the temporal evolution of median GSAT anomalies (**a**) and CO_2 concentrations (**b**). The right panels (**c**–**j**) summarize end-of-century outcomes (2099) with boxplots showing the median, interquartile range (25th–75th percentiles), and whiskers representing the 5th–95th percentiles, alongside histograms illustrating the full distributions (minimum to maximum).

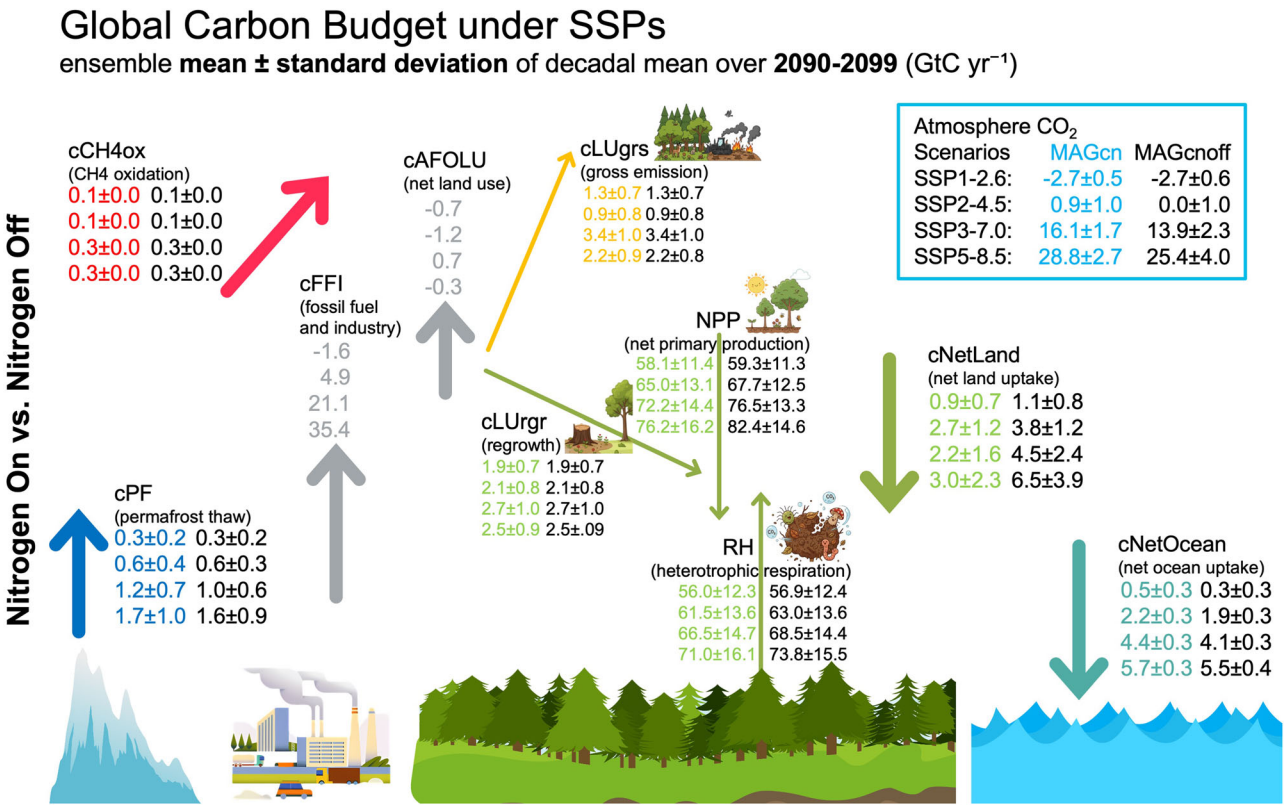

Fig. 2 | Reconstructed global carbon budget from MAGICC-CNit MAGcn and MAGcnoff ensemble projections under SSP scenarios. Colored values indicate the MAGcn ensemble, while black values indicate the MAGcnoff ensemble. Carbon emissions from fossil fuels and industry (cFFI) and from agriculture, forestry and other land use (cAFOLU) are prescribed inputs and therefore identical across ensembles (grey values). Values are shown as ensemble mean ± one standard deviation of decadal mean over 2090–2099.

SSP5-8.5 (Fig. 1c–f). Across these scenarios, the medians exceed those of the MAGcnoff ensemble by 0.16–0.25 °C and those of the MAGc ensemble by 0.09–0.16 °C. The full distributions of GSAT anomalies—including 5th and 95th percentiles and the minimum and maximum—also shift upward from MAGc and MAGcnoff to MAGcn.

For end-of-century CO_2 concentrations, the MAGcn ensemble projects 439.18 [415.14, 479.89] ppm for SSP1-2.6, 590.81 [560.91, 655.5] ppm for SSP2-4.5, 842.63 [795.8, 919.87] ppm for SSP3-7.0, and 1119.04 [1051.67, 1221.73] ppm for SSP5-8.5 (Fig. 1g–j). Across these scenarios, the medians are higher than MAGcnoff and MAGc by 15.32–57.04 ppm and 10.72–58.09 ppm, respectively. The 5th and 95th percentiles of CO_2 concentrations also shift upward, and ensemble distributions differ notably. The medians and 95th percentiles of MAGcnoff and MAGc are nearly identical (within 6 ppm), consistent with their similar warming medians, but their lower tails diverge substantially: MAGcnoff shows 5th percentile CO_2 concentrations ~30–70 ppm lower than MAGc, with differences increasing across scenarios.

Future global carbon budget under SSPs

The differences in GSAT anomalies and CO_2 concentrations among ensembles are primarily driven by reduced land carbon uptake (cNetLand, i.e., net atmosphere-to-land flux) when nitrogen is included (Fig. 2 and Supplementary Fig. S2). Under SSP5-8.5, the MAGcn ensemble projects an end-of-century decadal mean cNetLand of 3.0 ± 2.3 GtC yr^{-1}, less than half of the 6.5 ± 3.9 GtC yr^{-1} in MAGcnoff (Fig. 2). Nitrogen reduces mean cNetLand by 2.3, 1.1, and 0.2 GtC yr^{-1} under SSP3-7.0, SSP2-4.5, and SSP1-2.6, respectively. The standard deviation of cNetLand is smaller in MAGcn across all scenarios. Moreover, MAGcn projects negative 5th percentile cNetLand values under SSP3-7.0 and SSP5-8.5 (–0.5 and –0.9 GtC yr^{-1}; Supplementary Fig. S3), indicating a potential shift of land to a net carbon source by century's end in high-emission scenarios.

Examining cNetLand components, net primary production (NPP) in the MAGcn ensemble ranges from 58.1 to 76.2 GtC yr^{-1} across SSP1-2.6 to SSP5-8.5 (Fig. 2). These values are slightly lower than those in MAGcnoff by ~1–6 GtC yr^{-1} and markedly lower than those in MAGc by ~12–25 GtC yr^{-1}, depending on the emission scenario (Supplementary Fig. S2). The MAGcn ensemble also shows substantially reduced standard deviations of NPP relative to MAGc, consistent with narrower 5th–95th percentile ranges (e.g., 53.9–100.2 vs. 65.0–140.7 GtC yr^{-1} under SSP5-8.5; Supplementary Figs. S3 and S4), underscoring nitrogen as a strong constraint on NPP. Heterotrophic respiration (RH) shows a similar pattern, with smaller differences in end-of-century decadal means and comparable spreads (e.g., 56.0 ± 12.3 to 71.0 ± 16.1 GtC yr^{-1} in MAGcn vs. 56.9 ± 12.4 to 73.8 ± 15.5 GtC yr^{-1} in MAGcnoff across SSP1-2.6 to SSP5-8.5).

For land-use fluxes, both gross emissions (cLUgrs) and regrowth (cLUrgr) are about 0.5 GtC yr^{-1} lower in MAGcn than in MAGc (Supplementary Fig. S2), while their uncertainties remain comparable (standard deviation <1.1 GtC yr^{-1}; 5th–95th percentile range <2.5 GtC yr^{-1}; Supplementary Figs. S2–S4).

The ocean sequesters 0.5–5.7 GtC yr^{-1} in MAGcn via ocean carbon uptake (cNetOcean, i.e., net atmosphere-to-ocean flux), approximately 0.3 GtC yr^{-1} more than in MAGcnoff and MAGc for both medians and means (Fig. 2 and Supplementary Figs. S2–S4). Permafrost releases 0.3–1.7 GtC yr^{-1} through thaw emissions (cPF), with similar values across ensembles (differences <0.2 GtC yr^{-1} for medians and means). Methane oxidation contributes an identical (to within rounding) 0.1–0.3 GtC yr^{-1} across ensembles.

Aggregating all fluxes, the MAGcn ensemble projects mean end-of-century atmospheric CO_2 changes of –2.7 GtC yr^{-1} (–1.3 ppm yr^{-1}) under

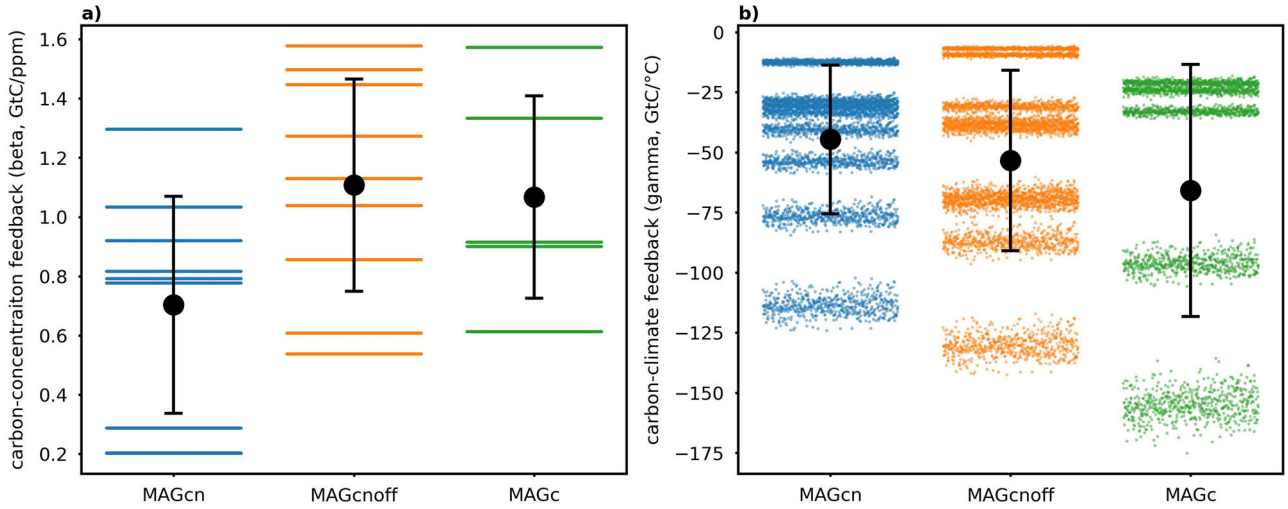

Fig. 3 | Uncertainty in land carbon cycle feedbacks diagnosed from the MAGICC-CNit ensembles. Land carbon–concentration (**a**) and carbon–climate (**b**) feedbacks derived from the MAGICC-CNit MAGcn, MAGcnoff, and MAGc ensembles, diagnosed from 1pctCO2 and 1pctCO2-bgc experiments (see "Methods"). The scatter points represent all ensemble members (600 climate members combined with 14 CMIP6 ESM-calibrated carbon-cycle parameter sets; see "Methods"). The variation in feedback strength is primarily driven by the carbon-cycle parameter sets, as reflected by the distinct clustered groups within each ensemble. Black dots and error bars indicate the ensemble mean and standard deviation. In MAGICC, temperature change is simulated as part of an emission–concentration–radiation–climate cascade[21]. In the 1pctCO2-bgc configuration, the radiation scheme is decoupled from CO_2, so no temperature response is produced. As a result, carbon–concentration feedbacks take discrete values corresponding to individual emulated CMIP6 ESMs (see "Methods"). By contrast, carbon–climate feedbacks are continuous. Each carbon-cycle parameter set is combined with MAGICC climate-response parameters, producing a distribution of temperature responses under the same CO_2 forcing and reflecting uncertainty in climate sensitivity.

Table 1 | Land carbon–concentration and carbon–climate feedbacks from MAGICC-CNit ensembles, with CNit v2.0 calibrated to CMIP6 ESMs

CNit v2.0 calibrated to CMIP6 ESMs	Carbon-concentration feedback (GtC ppm^{-1})			Carbon-climate feedback (GtC °C^{-1})		
	MAGcn	MAGcnoff	MAGc	MAGcn	MAGcnoff	MAGc
CNit(ACCESS-ESM1-5)	0.29	0.86	–	−30.60 ± 1.08	−67.89 ± 2.42	–
CNit(CESM2-WACCM)	0.92	1.13	–	−40.49 ± 1.64	−39.91 ± 1.65	–
CNit(CMCC-CM2-SR5)	0.20	0.61	–	−12.02 ± 0.47	−6.75 ± 0.37	–
CNit(CMCC-ESM2)	0.20	0.54	–	−12.79 ± 0.52	−9.41 ± 0.50	–
CNit(MIROC-ES2L)	1.30	1.50	–	−113.65 ± 3.91	−130.31 ± 4.50	–
CNit(MPI-ESM1-2-LR)	0.82	1.04	–	−53.80 ± 1.86	−70.63 ± 2.42	–
CNit(NorESM2-LM)	0.79	1.45	–	−33.37 ± 1.34	−37.34 ± 1.55	–
CNit(NorESM2-MM)	0.78	1.27	–	−28.33 ± 1.08	−30.76 ± 1.20	–
CNit(UKESM1-0-LL)	1.03	1.58	–	−76.51 ± 2.62	−87.16 ± 3.03	–
CNit(BCC-CSM2-MR)	–	–	1.57	–	–	−154.99 ± 5.94
CNit(CanESM5)	–	–	0.92	–	–	−20.96 ± 0.88
CNit(CanESM5-1)	–	–	0.90	–	–	−24.23 ± 1.06
CNit(CNRM-ESM2-1)	–	–	1.33	–	–	−96.15 ± 3.52
CNit(IPSL-CM6A-LR)	–	–	0.61	–	–	−32.98 ± 1.11
Ensemble mean	0.70	1.11	1.07	−44.62	−53.35	−65.86
Ensemble std	0.37	0.36	0.34	30.88	37.53	52.43

When combining the MAGc and MAGcn ensembles (i.e., all emulated CMIP6 ESMs), the carbon–concentration feedback is 0.83 ± 0.40 GtC ppm^{-1} and the carbon–climate feedback is −52.21 ± 41.21 GtC °C^{-1}.

– indicates not applicable because the emulated ESM is not part of the corresponding ensemble (see "Methods").

SSP1-2.6, +0.9 GtC yr^{-1} (+ 0.4 ppm yr^{-1}) under SSP2-4.5, +16.1 GtC yr^{-1} (+ 7.6 ppm yr^{-1}) under SSP3-7.0, and +28.8 GtC yr^{-1} (+ 13.6 ppm yr^{-1}) under SSP5-8.5. Without nitrogen, the MAGcnoff ensemble projects smaller changes of −2.7, +0.0, +13.9, and +25.4 GtC yr^{-1}, respectively.

Uncertainty of land carbon cycle feedbacks

The carbon–concentration feedback is 0.70 ± 0.37 GtC ppm^{-1} in MAGcn, 1.11 ± 0.36 GtC ppm^{-1} in MAGcnoff, and 1.07 ± 0.34 GtC ppm^{-1} in MAGc (ensemble mean ± standard deviation; Fig. 3a and Table 1). Across all emulated ESMs (combining MAGcn and MAGc), the strongest feedback

(1.57 GtC ppm^{-1}) occurs in CNit(BCC-CSM2-MR), a C-only ESM, while the weakest (0.20 GtC ppm^{-1}) appears in CNit(CMCC-CM2-SR5) and CNit(CMCC-ESM2), both CN-coupled models. The MAGcnoff maximum (1.58 GtC ppm^{-1}) arises from the nitrogen-off mode of CNit(UKESM1-0-LL), whereas the lowest (~0.60 GtC ppm^{-1}) remains in the CMCC model emulations. Across all emulated models, disabling nitrogen cycling systematically strengthens the carbon–concentration feedback (Table 1).

The carbon–climate feedback is weakest in MAGcn (−44.62 ± 30.88 GtC °C^{-1}, ensemble mean ± standard deviation; Fig. 3b and Table 1), followed by MAGcnoff (−53.35 ± 37.53 GtC °C^{-1}) and MAGc (−65.86 ± 52.43 GtC °C^{-1}). Among individual emulations, CNit(BCC-CSM2-MR) and CNit(MIROC-ES2L) show the strongest magnitudes (−154.99 ± 5.94 and −113.65 ± 3.91 GtC °C^{-1}, respectively), while the CMCC models exhibit the weakest (~−12 GtC °C^{-1}). Other ESM emulations range from −100 to −20 GtC °C^{-1}. Disabling nitrogen generally amplifies the carbon–climate feedback, except in CNit(CMCC-CM2-SR5), CNit(CMCC-ESM2), and CNit(CESM2-WACCM).

Discussion

This study synthesizes emission-driven, probabilistic projections of fully coupled climate–carbon–nitrogen dynamics under the four Tier-1 ScenarioMIP SSPs using MAGICC-CNit, implemented within a self-consistent framework that emulates CMIP6 ESMs (see Supplementary Discussion S1, RCM vs. ESM projections) and enables quantification and isolation of nitrogen effects independent of structural differences (see Methods). While our analysis primarily addresses end-of-century outcomes, near-term evaluation against the Global Carbon Budget 2024 (GCB2024)[25] demonstrates that MAGICC-CNit projections are consistent with GCB2024 estimates once methodological differences are accounted for (Supplementary Fig. S5 and Supplementary Discussion S2). This agreement reinforces confidence in the model's representation of the coupled climate–carbon system across the historical-to-contemporary transition.

Across scenarios, including an active nitrogen cycle (MAGcn vs. MAGcnoff, excluding structural differences) consistently produces a very likely (shifted 5th–95th percentiles) warmer future with higher atmospheric CO_2 concentrations (median increases of 0.16–0.25 °C and 15.32–57.04 ppm, respectively; Fig. 1). Median GSAT anomalies exceed 1.5 °C in all SSPs and remain below 2.0 °C only in SSP1-2.6, consistent with concentration-driven CMIP6 results[26]. In SSP1-2.6, peak warming—including median and 5th–95th percentiles—shifts upward when nitrogen is included (e.g., 1.90 vs. 1.79 °C for medians; Supplementary Fig. S6). The divergence between MAGcn and MAGcnoff median projections increases over time, reflecting stronger nitrogen limitation and consistent with historical global declines in foliar nitrogen[27,28]. The divergence is more pronounced under high-emission scenarios, suggesting that nitrogen limitation acts as a positive feedback on warming[9,29], consistent with the largely reduced carbon–concentration feedback and less negative carbon-climate feedback (Table 1). End-of-century CO_2 distributions also differ markedly between MAGcn and MAGcnoff, highlighting substantial variation in nitrogen effects on the carbon cycle across CN-coupled ESMs.

The amplified warming and higher CO_2 levels in MAGcn relative to MAGcnoff are primarily driven by reduced net land carbon uptake (cNetLand), particularly under high-emission scenarios (3.0 ± 2.3 vs. 6.5 ± 3.9 GtC yr^{-1} in SSP5-8.5; Fig. 2). In SSP3-7.0 and SSP5-8.5, the 5th percentile of cNetLand turns negative (−0.5 and −0.9 GtC yr^{-1}), indicating a risk of land becoming a net carbon source under high emissions—a consequence of nitrogen limitation and climate–carbon–nitrogen interactions[1]. Comparison with MAGc further shows that including the nitrogen cycle reduces cNetLand by up to 2.4 GtC yr^{-1} under SSP5-8.5 (Fig. 2 and Supplementary Fig. S2). However, differences between MAGcn and MAGc also reflect structural differences between CN-coupled and C-only ESMs (e.g., varying land-use emissions), complicating attribution of the nitrogen effect (see details in Supplementary Discussion S2).

Given that land-use component is identical in MAGcn and MAGcnoff, the observed reductions in cNetLand arise from declines in both NPP and RH, with NPP declining more strongly (Fig. 2 and Supplementary Fig. S1). Consequently, net ecosystem production (NEP, i.e., NPP–RH) decreases, consistent with studies showing NEP overestimation in C-only ESMs[30]. Nitrogen inclusion reduces terrestrial carbon–cycle feedbacks in CMIP6 ESMs[11], improves simulations of photosynthesis and global net biome production (equivalent to cNetLand;[12]), and constrains NPP[19,31,32], explaining the substantial reductions in both median/mean values and spread of NPP and RH in MAGcn relative to MAGc across scenarios (Fig. 2 and Supplementary Fig. S1) and supported by diagnosed feedback metrics (Fig. 3 and Table 1).

Comparisons between MAGcnoff and MAGc reveal similar GSAT and CO_2 patterns, with slightly higher warming and CO_2 in MAGc (Fig. 1). This indicates that C-only ESMs do not represent CN-coupled ESMs with unlimited nitrogen availability. Beyond nitrogen effects, differences in model representation and parameterization between C-only and CN-coupled ESMs contribute to divergent warming projections. This aligns with previous CNit results showing CO_2 fertilization is artificially enhanced to compensate for missing nitrogen deposition and fertilization[20], as well as with evidence from dynamic global vegetation models indicating that calibrating terrestrial carbon uptake to the historical sink can create a disconnect between simulated carbon and nitrogen cycling processes[33].

For the multi-model mean combining all ESMs, we find a weaker carbon–concentration feedback and stronger carbon–climate feedback compared with earlier results (0.83 ± 0.40 GtC ppm^{-1} and −52.21 ± 41.21 GtC °C^{-1} with 14 ESMs here vs. 0.97 ± 0.40 GtC ppm^{-1} and −45.1 ± 50.6 GtC °C^{-1} with 11 ESMs in ref. 11). This difference primarily reflects inclusion of CNit(CMCC-CM2-SR5) and CNit(CMCC-ESM2), which exhibit the smallest feedbacks (~0.2 GtC ppm^{-1} and −12 GtC °C^{-1}; Table 1), highlighting substantial uncertainty in carbon cycle feedbacks across CMIP6 ESMs.

The carbon–concentration feedback is 37% weaker in MAGcn than in MAGcnoff (0.70 ± 0.37 vs. 1.11 ± 0.36GtC ppm^{-1}), with all emulated ESMs showing the same direction. This confirms that nitrogen primarily limits CO_2 fertilization[3,18,27,34]. In contrast, the mean carbon–concentration feedback is nearly identical in MAGcnoff and MAGc, indicating that MAGICC-CNit effectively constrains nitrogen effects on CO_2-driven processes represented in the emulated ESMs and increasing confidence in the MAGcnoff diagnosis.

The carbon–climate feedback in MAGcn is −44.62 GtC °C^{-1}, 16% weaker than in MAGcnoff and 32% weaker than in MAGc (Table 1). The enhanced carbon-climate feedback from MAGcn to MAGcnoff reflects that warming and increased substrate trigger a respiration surge that outpaces NPP gains from disabling nitrogen limitation. Conversely, the weakened feedback seen in CNit(CMCC-CM2-SR5), CNit(CMCC-ESM2), and CNit(CESM2-WACCM) results from the lack of strong nitrogen-driven enhancement on soil respiration (i.e., recalcitrant soil organic matter decomposition) when nitrogen is disabled. This dynamic also explains the marginally enhanced feedback in the two NorESM models, where the dampening of soil respiration is slightly outweighed by a substantial surge in litter production (i.e., providing more substrate for decomposition) once its nitrogen limitation is removed. Ultimately, this bi-directional shift in carbon-climate feedback strength highlights the substantial uncertainty inherent to representations and parameterizations of the nitrogen cycle and carbon-nitrogen coupling in current ESMs[9,10,18,34,35].

The stronger carbon-climate feedback in MAGc explains the lower warming and CO_2 concentrations in MAGcnoff compared with MAGc (Fig. 1). Because both configurations lack active nitrogen, differences in their feedback means and standard deviations stem from residual model formulation, parameterization, and historical tuning between CN-coupled and C-only ESMs rather than nitrogen constraints. This cautions that discrepancies between CN-coupled and C-only ESMs cannot be attributed solely to nitrogen inclusion, emphasizing the need to jointly recalibrate integrated carbon-nitrogen systems instead of simply merging separately tuned subsystems.

With its demonstrated effective emulation of state-of-the-art ESM behavior, MAGICC-CNit provides a synthesis of global mean temperature, atmospheric CO_2, and global carbon budgets under scenarios in a self-consistent manner, where all physical components operate within the same framework and are driven by emissions. This self-consistency enables integration of information from the GCB estimates, CMIP assessments, and observations (not shown here but representing the logical next step for constructing a Bayesian ensemble) without violating fundamentals such as mass conservation, which can be difficult when combining results from different models (e.g., the mass imbalance in the GCB estimates). The framework also allows for direct comparison of the emulated ESMs, which is challenging in CMIP ensembles due to differences in process representation and model structure. The shift in CMIP7 toward emission-driven experiments highlights the increasing emphasis on self-consistency in ESM modeling practice (see Supplementary Discussion S1).

Using this framework, the fully coupled climate–carbon–nitrogen dynamics show that terrestrial nitrogen limitation substantially reduces land carbon uptake, weakens carbon–climate feedbacks, increases atmospheric CO_2 concentrations, and amplifies global warming, with high-emission scenarios indicating a likelihood of land becoming a net carbon source by 2100. C-only ESMs implicitly capture some historical nitrogen effects but fail to represent their full impact on future projections. The global carbon budget under these scenarios provides the first comprehensive quantification of the future carbon cycle. These findings highlight the critical importance of explicitly coupling nitrogen cycling in ESMs and emulators to produce robust climate-carbon cycle projections and demonstrate the value of a self-consistent, physically based emulation framework for advancing future climate assessments.

Methods

MAGICC-CNit model and ensemble

MAGICC is one of the most widely used reduced-complexity models (RCMs, also referred to as simple climate models) and has been continuously updated since its inception[36–38]. For example, MAGICC6 introduces variable climate sensitivities and an updated carbon cycle[21], while MAGICC7 incorporates an updated sea level model[39], improvements to radiative forcing schemes, the new permafrost module[40] and Arctic sea ice emulator[41], among other enhancements. One of the most significant recent updates is the integration of the coupled carbon–nitrogen cycle model, CNit[19], developed in response to the increased number of CMIP6 ESMs that include a nitrogen cycle. CNit is a global box model based on first-order decay that simulates major carbon–nitrogen fluxes and pools, with key processes influenced by climate, land use, and nitrogen status. It integrates carbon and nitrogen cycle components that can be coupled or decoupled through a structural nitrogen switch, allowing it to emulate both C-only and CN-coupled ESMs and to isolate nitrogen effects independent of model structural differences. The latest version, CNit v2.0, is calibrated against CMIP6 ESMs across historical, idealized, and SSP scenarios, effectively reproducing diverse carbon–nitrogen cycle dynamics[20].

The probabilistic distribution of MAGICC7 (v7.5.3, with 600 members) has been calibrated to capture the relationship between emissions and global surface air temperature (GSAT) change. This calibration incorporates the assessed uncertainty in equilibrium climate sensitivity (ECS), transient climate response (TCR), historical GSAT changes, effective radiative forcing (ERF), carbon cycle metrics, and future warming projections under the concentration-driven SSP scenarios, as assessed by IPCC AR6 WG1[24,42]. We refer to the MAGICC v7.5.3 ensemble as MAGv7.

With the latest version of MAGICC (MAGICC v7.5.3 with CNit v2.0, hereafter MAGICC-CNit), we use 14 calibrated parameter sets, each representing the best fit to one of 14 CMIP6 ESMs (9 CN-coupled and 5 C-only). The number of calibrated models is limited by the availability of complete and reliable carbon–nitrogen cycle outputs required for training[20,43]. Each CNit-emulated ESM is paired with 600 ensemble members for climate response, radiative forcing, and other gas-cycle parameters from MAGv7. This results in two ensembles: one using C-only ESM emulations ($5 \times 600 = 3000$ members, referred to as MAGc) and another using CN-coupled ESM emulations ($9 \times 600 = 5400$ members, referred to as MAGcn). We also run the nitrogen-off configuration for CN-coupled models (MAGcnoff, where nitrogen does not affect carbon dynamics) for direct separation of the nitrogen effect. Consequently, MAGc, MAGcn, and MAGcnoff differ only in their carbon–nitrogen parameter values—reflecting the emulated C-only ESMs, the emulated CN-coupled ESMs, and the emulated CN-coupled ESMs with deactivated carbon–nitrogen coupling, respectively. Thus, comparing MAGc and MAGcn highlights the structural differences between ESMs with and without a nitrogen cycle, while comparing MAGcn and MAGcnoff disentangles the nitrogen effect independent of those broader model structural differences.

MAGICC-CNit emission-driven SSP projection

We run the various MAGICC-CNit ensembles from 1850 to 2100 for the four Tier-1 experiments in CMIP6 ScenarioMIP: SSP1-2.6, SSP2-4.5, SSP3-7.0, and SSP5-8.5[14]. The emission-driven simulations begin in 2015, which marks the start of the projection period for CMIP6. These simulations incorporate full emissions for 43 greenhouse gases (e.g., CO_2, CH_4, and N_2O; using both total and sector-specific emissions where available), based on data from the SSP Public Database Version 2.0 (https://tntcat.iiasa.ac.at/SspDb, last accessed 22 June 2025)[22,44].

The SSP database provides emissions data for 2015, 2020, and then at ten-year intervals up to 2100. For years in between, we apply linear interpolation to estimate annual values. Historical emissions are sourced from the Reduced Complexity Model Intercomparison Project (RCMIP)[23], incorporating data from the Community Emissions Data System, Global Carbon Budget, PRIMAP-hist, World Meteorological Organization, and atmospheric inversions.

Before the simulation year 2015, MAGICC-CNit operates in concentration-driven mode; thus, emissions do not affect concentrations between 1850 and 2015. Historical land use emissions are included in the CNit carbon cycle simulation and impact the terrestrial carbon cycle prior to 2015, but these effects are not interactive with atmospheric CO_2 over this period.

In addition to emissions, CNit requires nitrogen forcings, including atmospheric nitrogen deposition and fertilizer application. We use CMIP6 forcing datasets (input4MIPs) for the entire period from 1850 to 2100. Specifically, the sum of dry and wet deposition over land for both NHx and NOy species is used as the nitrogen deposition input[45], and fertilizer application data are taken from the Land-Use Harmonization (LUH2) management dataset[46], consistent with the CNit v2.0 calibration.

To separately calculate carbon-concentration and carbon-climate feedback metrics, we run 1pctCO2 and 1pctCO2-bgc (CO_2 affects biogeochemistry only, not radiation) experiments with the MAGICC-CNit ensemble, both of which are driven by prescribed CO_2 concentration with a 1% increment every year until quadrupled (i.e., a 140-year simulation), and other gases are kept constant at the pre-industrial level. The selection of these two experiments allows for direct comparison with existing studies (Arora et al.[11]). These experiments are also included in the CNit v2.0 calibration.

Data availability

The source data of the ensemble projections are archived in Zenodo at https://doi.org/10.5281/zenodo.17748790[47].

Code availability

The MAGICC model source code is available at https://gitlab.com/magicc/magicc (MAGICC Development Team, 2025). The CNit model description and calibration are provided in our previous publications[19,20], and the source code is available at https://doi.org/10.5281/zenodo.15569386[48] and https://github.com/gangtang-au/cnit.

Received: 16 December 2025; Accepted: 1 June 2026;
Published online: 08 June 2026

References

1. Wieder, W. R., Cleveland, C. C., Smith, W. K. & Todd-Brown, K. Future productivity and carbon storage limited by terrestrial nutrient availability. *Nat. Geosci.* **8**, 441–444 (2015).
2. Thornton, P. E., Lamarque, J. -F., Rosenbloom, N.A. & Mahowald, N.M. Influence of carbon-nitrogen cycle coupling on land model response to CO_2 fertilization and climate variability. *Global Biogeochem. Cycles* **21**, 4 (2007).
3. LeBauer, D. S. & Treseder, K. K. Nitrogen limitation of net primary productivity in terrestrial ecosystems is globally distributed. *Ecology* **89**, 371–379 (2008).
4. Gruber, N. & Galloway, J. N. An Earth-system perspective of the global nitrogen cycle. *Nature* **451**, 293–296 (2008).
5. Sokolov, A. P. et al. Consequences of considering carbon–nitrogen interactions on the feedbacks between climate and the terrestrial carbon cycle. *J. Clim.* **21**, 3776–3796 (2008).
6. Zaehle, S. et al. Carbon and nitrogen cycle dynamics in the O-CN land surface model: 2. Role of the nitrogen cycle in the historical terrestrial carbon balance. *Global Biogeochem. Cycles* **24**, 1 (2010).
7. Meyerholt, J., Sickel, K. & Zaehle, S. Ensemble projections elucidate effects of uncertainty in terrestrial nitrogen limitation on future carbon uptake. *Glob. Change Biol.* **26**, 3978–3996 (2020).
8. Wiltshire, A. J. et al. JULES-CN: a coupled terrestrial carbon–nitrogen scheme (JULES vn5.1). *Geosci. Model Dev.* **14**, 2161–2186 (2021).
9. Zaehle, S. & Dalmonech, D. Carbon–nitrogen interactions on land at global scales: current understanding in modelling climate biosphere feedbacks. *Curr. Opin. Environ. Sustain.* **3**, 311–320 (2011).
10. Davies-Barnard, T. et al. Nitrogen cycling in CMIP6 land surface models: progress and limitations. *Biogeosciences* **17**, 5129–5148 (2020).
11. Arora, V. K. et al. Carbon–concentration and carbon–climate feedbacks in CMIP6 models and their comparison to CMIP5 models. *Biogeosciences* **17**, 4173–4222 (2020).
12. Gier, B. K. et al. Representation of the terrestrial carbon cycle in CMIP6. *Biogeosciences* **21**, 5321–5360 (2024).
13. Eyring, V. et al. Overview of the Coupled Model Intercomparison Project Phase 6 (CMIP6) experimental design and organization. *Geosci. Model Dev.* **9**, 1937–1958 (2016).
14. O'Neill, B. C. et al. The Scenario Model Intercomparison Project (ScenarioMIP) for CMIP6. *Geosci. Model Dev.* **9**, 3461–3482 (2016).
15. Forsmark, B., Nordin, A., Maaroufi, N. I., Lundmark, T. & Gundale, M. J. Low and high nitrogen deposition rates in northern coniferous forests have different impacts on aboveground litter production, soil respiration, and soil carbon stocks. *Ecosystems* **23**, 1423–1436 (2020).
16. Hedin, L. O, Brookshire, E. N. J., Menge, D. N. L. & Barron, A. R. The nitrogen paradox in tropical forest ecosystems. *Ann. Rev. Ecol. Evol. System.* **40**, 613–635 (2005).
17. Kraiser, T., Gras, D. E., Gutiérrez, A. G., González, B. & Gutiérrez, R. A. A holistic view of nitrogen acquisition in plants. *J. Exp. Bot.* **62**, 1455–1466 (2011).
18. Zaehle, S. et al. Evaluation of 11 terrestrial carbon–nitrogen cycle models against observations from two temperate free-air CO_2 enrichment studies. *N. Phytol.* **202**, 803–822 (2014).
19. Tang, G., Nicholls, Z., Norton, A., Zaehle, S. & Meinshausen, M. Synthesizing global carbon–nitrogen coupling effects – the MAGICC coupled carbon–nitrogen cycle model v1.0. *Geosci. Model Dev.* **18**, 2193–2230 (2025).
20. Tang, G. et al. Understanding the drivers of carbon–nitrogen cycle variability in CMIP6 ESMs with MAGICC CNit v2.0: model and calibration updates. *J. Adv. Model. Earth Syst.* **18**, e2025MS005270 (2026).
21. Meinshausen, M., Raper, S. C. B. & Wigley, T. M. L. Emulating coupled atmosphere-ocean and carbon cycle models with a simpler model, MAGICC6 – Part 1: model description and calibration. *Atmos. Chem. Phys.* **11**, 1417–1456 (2011).
22. Riahi, K. et al. The Shared Socioeconomic Pathways and their energy, land use, and greenhouse gas emissions implications: an overview. *Glob. Environ. Change* **42**, 153–168 (2017).
23. Nicholls, Z. et al. Reduced complexity model intercomparison project phase 2: synthesizing earth system knowledge for probabilistic climate projections. *Earth's. Future* **9**, e2020EF001900 (2021).
24. Nicholls, Z. et al. Changes in IPCC scenario assessment emulators between SR1.5 and AR6 unraveled. *Geophys. Res. Lett.* **49**, e2022GL099788 (2022).
25. Friedlingstein, P. et al. Global carbon budget 2024. *Earth Syst. Sci. Data* **17**, 965–1039 (2025).
26. Tebaldi, C. et al. Climate model projections from the Scenario Model Intercomparison Project (ScenarioMIP) of CMIP6. *Earth Syst. Dynam.* **12**, 253–293 (2021).
27. Wang, S. et al. Recent global decline of CO2 fertilization effects on vegetation photosynthesis. *Science* **370**, 1295–1300 (2020).
28. Craine, J. M. et al. Isotopic evidence for oligotrophication of terrestrial ecosystems. *Nat. Ecol. Evol.* **2**, 1735–1744 (2018).
29. Zaehle, S., Friedlingstein, P. & Friend, A. D. Terrestrial nitrogen feedbacks may accelerate future climate change. *Geophys. Res. Lett.* **37**, 1 (2010).
30. Qiu, H., Hao, D., Zeng, Y., Zhang, X. & Chen, M. Global and northern-high-latitude net ecosystem production in the 21st century from CMIP6 experiments. *Earth Syst. Dynam.* **14**, 1–16 (2023).
31. Goll, D. S. et al. Nutrient limitation reduces land carbon uptake in simulations with a model of combined carbon, nitrogen and phosphorus cycling. *Biogeosciences* **9**, 3547–3569 (2012).
32. Thomas, R. Q., Brookshire, E. N. J. & Gerber, S. Nitrogen limitation on land: how can it occur in Earth system models?. *Glob. Change Biol.* **21**, 1777–1793 (2015).
33. Kou-Giesbrecht, S. et al. Evaluating nitrogen cycling in terrestrial biosphere models: a disconnect between the carbon and nitrogen cycles. *Earth Syst. Dynam.* **14**, 767–795 (2023).
34. Thomas, R. Q., Zaehle, S., Templer, P. H. & Goodale, C. L. Global patterns of nitrogen limitation: confronting two global biogeochemical models with observations. *Glob. Change Biol.* **19**, 2986–2998 (2013).
35. Davies-Barnard, T., Zaehle, S. & Friedlingstein, P. Assessment of the impacts of biological nitrogen fixation structural uncertainty in CMIP6 earth system models. *Biogeosciences* **19**, 3491–3503 (2022).
36. Wigley, T. M. L. & Raper, S. C. B. Thermal expansion of sea water associated with global warming. *Nature* **330**, 127–131 (1987).
37. Wigley, T. M. L. & Raper, S. C. B. Implications for climate and sea level of revised IPCC emissions scenarios. *Nature* **357**, 293–300 (1992).
38. Wigley, T. M. L. & Raper, S. C. B. Interpretation of high projections for global-mean warming. *Science* **293**, 451–454 (2001).
39. Nauels, A., Meinshausen, M., Mengel, M., Lorbacher, K. & Wigley, T. M. L. Synthesizing long-term sea level rise projections – the MAGICC sea level model v2.0. *Geosci. Model Dev.* **10**, 2495–2524 (2017).
40. Meinshausen, M. et al. The shared socio-economic pathway (SSP) greenhouse gas concentrations and their extensions to 2500. *Geosci. Model Dev.* **13**, 3571–3605 (2020).
41. Chilcott, S. M., Meinshausen, M. & Notz, D. SASIEv.1: a framework for seasonal and multi-centennial Arctic sea ice emulation. *Geosci. Model Dev.* **18**, 4965–4982 (2025).
42. Forster, P. et al. The Earth's energy budget, climate feedbacks, and climate sensitivity. in *Climate Change 2021: The Physical Science Basis. Contribution of Working Group I to the Sixth Assessment Report of the Intergovernmental Panel on Climate Change* (eds Masson-Delmotte, V., Zhai, P., Pirani, A., Connors, S. L., Péan, C., Berger, S. et al.) 923–1054 (Cambridge University Press, 2021).
43. Tang, G. et al. Investigating carbon and nitrogen conservation in reported CMIP6 Earth system model data. *Geosci. Model Dev.* **18**, 2111–2136 (2025).

44. Gidden, M. J. et al. Global emissions pathways under different socioeconomic scenarios for use in CMIP6: a dataset of harmonized emissions trajectories through the end of the century. *Geosci. Model Dev.* **12**, 1443–1475 (2019).
45. Hegglin, M., Kinnison, D. & Lamarque, J.-F. *CCMI Nitrogen Surface Fluxes in Support of CMIP6 - version 2.0.* (Earth System Grid Federation, 2016).
46. Hurtt, G. C. et al. Harmonization of global land use change and management for the period 850–2100 (LUH2) for CMIP6. *Geosci. Model Dev.* **13**, 5425–5464 (2020).
47. Tang, G. MAGICC-CNit probabilistic cross-ESM projection results for ScenarioMIP-CMIP6 Tier-1 SSPs. Zenodo 3461–3482 https://doi.org/10.5281/zenodo.17748791 (2025).
48. Tang, G. et al. Model source code for the MAGICC coupled carbon–nitrogen cycle model – CNit. Zenodo https://doi.org/10.5281/zenodo.15569387 (2025).

Acknowledgements

G.T. acknowledges support from the Dr Albert Shimmins Fund (Dr Albert Shimmins Postgraduate Writing-Up Award 2025), The University of Melbourne (Science Abroad Travelling Scholarships from the Faculty of Science and Graduate Researcher Travelling Funds from the School of Geography, Earth and Atmospheric Sciences), and the Max Planck Institute for Biogeochemistry (Guest Program). S.Z., T.G., and Z.N. acknowledge funding from the European Union's Horizon 2020 research and innovation programme (ESM2025, grant no. 101003536). Tilo Ziehn and Malte Meinshausen acknowledge support from the National Environmental Science Program (Climate Systems Hub), funded by the Australian Government Department of Climate Change, Energy, the Environment, and Water. The authors express our sincere gratitude to the World Climate Research Programme (WCRP), the Coupled Model Intercomparison Project Phase 6 (CMIP6), the Earth system model (ESM) groups, the Coupled Climate–Carbon Cycle Model Intercomparison Project (C4MIP) and related MIPs, and the Earth System Grid Federation (ESGF) for their invaluable collaborative efforts in making ESM outputs openly available and accessible.

Author contributions

G.T. and M.M. conceptualized the initial idea of developing the MAGICC-CNit projections for the ScenarioMIP SSPs. G.T. designed and calibrated CNit v2.0 and implemented it into MAGICC (updating MAGICC to MAGICC-CNit), with technical support from Z.N. A.N., T.G., Z.N., T.Z., S.Z., and M.M. contributed to the interpretation and in-depth discussion of the results. G.T., S.Z., Z.N., T.G., T.Z., and M.M. were responsible for funding acquisition. M.M., Z.N., and A.N. supervised the project. G.T. conducted the analysis, interpreted the results, and wrote the first draft of the manuscript. All authors contributed to reviewing and revising the manuscript.

Funding

G.T. discloses support from the Dr Albert Shimmins Fund [Dr Albert Shimmins Postgraduate Writing-Up Award 2025], The University of Melbourne [Science Abroad Travelling Scholarships from the Faculty of Science and Graduate Researcher Travelling Funds from the School of Geography, Earth and Atmospheric Sciences], and the Max Planck Institute for Biogeochemistry [Guest Program]. S.Z., T.G., and Z.N. disclose support from the European Union [Horizon 2020 research and innovation programme (ESM2025, grant no. 101003536)]. T.Z. and M.M. acknowledge support from the Australian Government Department of Climate Change, Energy, the Environment, and Water [National Environmental Science Program (Climate Systems Hub)]. Open Access funding enabled and organized by Projekt DEAL.

Competing interests

The authors declare no competing interests.

Additional information

Supplementary information The online version contains supplementary material available at https://doi.org/10.1038/s43247-026-03736-0.

Correspondence and requests for materials should be addressed to Gang Tang.

Peer review information *Communications Earth and Environment* thanks the anonymous reviewers for their contribution to the peer review of this work. Primary Handling Editors: Huai Chen and ChenRui Diao. A peer review file is available.

Reprints and permissions information is available at http://www.nature.com/reprints

Publisher's note Springer Nature remains neutral with regard to jurisdictional claims in published maps and institutional affiliations.

Open Access This article is licensed under a Creative Commons Attribution 4.0 International License, which permits use, sharing, adaptation, distribution and reproduction in any medium or format, as long as you give appropriate credit to the original author(s) and the source, provide a link to the Creative Commons licence, and indicate if changes were made. The images or other third party material in this article are included in the article's Creative Commons licence, unless indicated otherwise in a credit line to the material. If material is not included in the article's Creative Commons licence and your intended use is not permitted by statutory regulation or exceeds the permitted use, you will need to obtain permission directly from the copyright holder. To view a copy of this licence, visit http://creativecommons.org/licenses/by/4.0/.

© The Author(s) 2026